The North American Society (NASTT) and the
International Society for Trenchless Technology (ISTT)
International No-Dig Show 2009

Toronto, Ontario Canada
March 29 – April 3, 2009

Paper B-1-02

HYDRAULIC FRACTURE EXPERIMENTS IN SAND AND GRAVEL AND APPROXIMATIONS FOR MAXIMUM ALLOWABLE MUD PRESSURE

David Elwood[1] and Ian Moore[2]

[1] Thurber Engineering Ltd., Oakville ON
[2] GeoEngineering Centre, Queen's University, Kingston, ON

ABSTRACT: Directional drilling uses pressurized mud when drilling through fluvial and glaciofluvial materials to maintain borehole stability and remove cuttings. Failure of the soil surrounding the borehole is controlled by the shear strength of this frictional ground and this influences the maximum allowable mud pressure that may be applied to the borehole. While there have been a number of theoretical studies of mud loss mechanisms, there have been few if any experimental investigations to examine the efficacy of the proposed design equations.

A horizontal directionally drilled borehole is examined in the laboratory using experiments in a uniformly graded sand and a layered sand and gravel system. Measurements of mud pressure and surface displacements associated with blowout are compared to analytical calculations. During the experiments, the downhole mud pressures to determine the borehole pressure that leads to mud loss and surface displacements were measured. Physical information obtained during the experiments was used to assess the effectiveness of various analytical models to estimate the mud loss pressures and displacements. Use of the existing analytical solutions was found to be questionable (unconservative) during pilot borehole drilling (the configuration studied in these experiments).

1. INTRODUCTION

During directional drilling through sands and gravels such as fluvial and glaciofluvial deposits, bentonite based fluids are pumped into the borehole to remove cuttings and to provide stability to the borehole walls. Excessive mud pressures can result in shear failure of the soil in the vicinity of the borehole resulting in a localised loss of fluid circulation and a breach of mud at the ground surface. To date, the maximum allowable fluid pressure has been estimated using analytical models with little to no known physical data to confirm the efficacy of the state-of-the-art methods. In addition, there has been no known research regarding the estimation of the displacement of the ground surface associated with mud loss or measurement of the actual displacements during borehole failure.

The current state-of-the-art method for estimating the allowable fluid pressures was first described by Lugar and Hergarden (1988) and later by Keulen et al. (2001) and is commonly referred to as the Delft Solution. The US Army Corps of Engineers has adopted this theory as a guideline to practitioners responsible for the design of horizontal drilled boreholes (Conroy et al. 2002a,b) and is considered applicable to a wide variety of soils.

In order to help designers and contractors alike minimize the likelihood for fluid loss and ground heave during HDD projects carried out in sands and gravels, laboratory experiments were designed to model a horizontally drilled borehole that was loaded to failure with a bentonite slurry, and the results have been compared with existing analytical models.

2. EXISTING THEORIES

Current state-of-the-art theories to estimate the maximum internal borehole pressure suggest that the material may be defined by assuming that the material is an infinite elastic-plastic solid, it has uniform vertical and horizontal stresses, uniform elastic modulus, Poisson's ratio, and shear strength dictated by the Mohr-Coulomb failure criterion, and that there is zero volume change within the plastic zone (dilation angle is zero). Finally it is assumed that the increase of internal pressure is from a uniform radial borehole pressure and that the solution is valid for a finite depth borehole. Current theories are based on the expansion of a pre-existing cylindrical opening as described by Vesić (1972). The Delft equation, which defines the maximum internal borehole fluid pressure, is generally accepted as the current state-of-the-art practice, and is shown below as Equation 1. This approach is based on the assumption that mud loss through the surrounding soil occurs once the radius of the plastic zone in the cavity expansion solution is calculated to extend as far as the ground surface.

$$p_{max} = (p'_f + c\cot\phi)\cdot[(\frac{R_o}{R_{pmax}})^2 + Q]^{\frac{-\sin\phi}{1+\sin\phi}} - c\cot\phi \qquad \text{[Eq.1]}$$

where; $Q = (\sigma'_o \cdot \sin\phi + c\cdot\cos\phi)/G$;

p_{max} is the maximum internal pressure;
p'_f is defined as $[\sigma'_o(1+\sin\phi) + (c\cos\phi)] - u$;
R_o is the initial borehole radius;
R_{pmax} is the maximum plastic radius;
G is the shear modulus of the material;
σ'_o is the initial vertical overburden pressure; and
c is the cohesion of the soil.

Lugar and Hergarden (1988) and Keulen et al. (2001) use different definitions for the limiting internal pressure or the allowable internal fluid pressure that prevents failure of the surrounding soil mass and loss of drilling mud. Lugar and Hergarden (1988) defined the limiting pressure as 90% of the maximum internal pressure for a purely cohesive material (saturated fine grained soils responding in an undrained condition). The maximum pressure was defined as a plastic radius (R_{pmax}) equal to the total depth of soil cover measured from the crown of the borehole to the ground surface. In contrast, Keulen et al. (2001) defined the limiting pressure for a cohesive frictional material as the internal borehole pressure which corresponds to a maximum plastic radius (R_{pmax}) equal to two thirds of the depth of soil cover (two thirds of the distance from the crown of the borehole to the ground surface). A full scale experiment carried out by Lugar and Hergarden (1988) reported good correlations of the actual downhole pressures during fluid loss with those estimated using both Equation 1 and numerical modelling.

Other more complex cavity expansion theories which consider the deformations of the material within the elastic zone and the influence of the angle of dilation within the material undergoing shear failure are also available. Theories for cavity expansion provided by Carter, Booker and Yeung (1986) and by Yu and Houlsby (1991) were investigated and the validity of these theories was evaluated through comparison with the experimental results.

3. EXPERIMENTS

3.1 TEST PIT AND SOIL PREPARATION

The experiments were conducted in a rectangular concrete pit 2m wide, 2m long, and 1.5m deep, Figure 1. The tests featured an additional 0.6m of borehole length through a recess at one end, as shown on Figure 1, making the total length of the test pit in the direction of the borehole 2.6m.

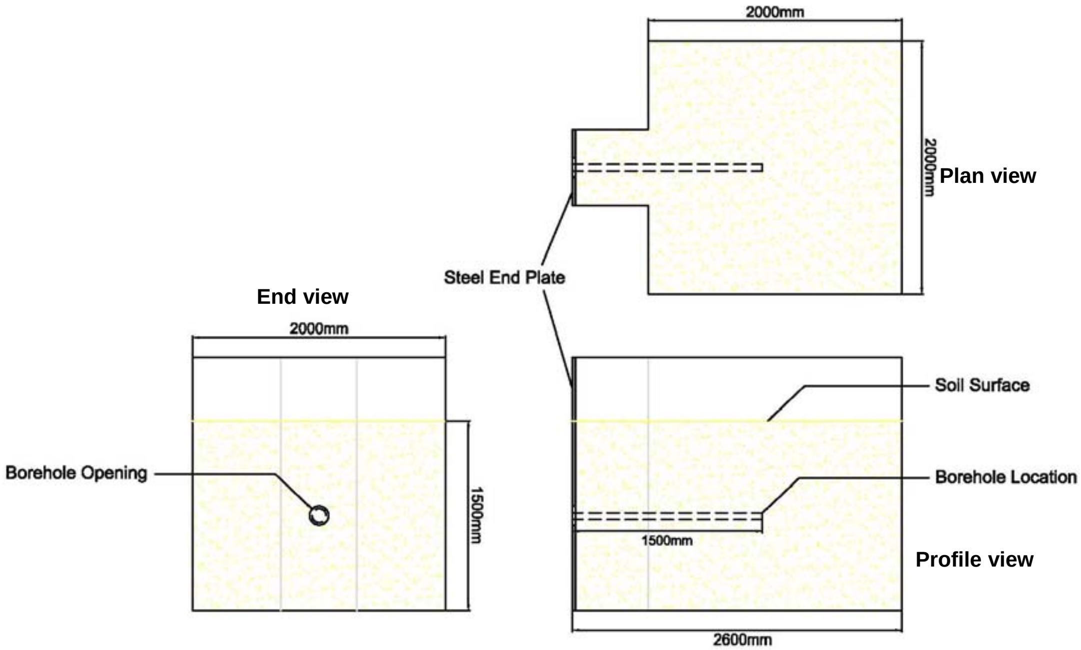

Figure 1 Test pit configuration

Five experiments were conducted in the concrete pit. Of the five experiments, three were carried out in sand, and two were undertaken with the upper 300mm of sand replaced with a well graded sand and gravel mixture similar to a material designated 'Granular A' in Ontario (GW-SW according to the Unified Classification System). The purpose of the layered soils was two-fold, first, to help understand the impact of layered granular systems like those used for roadways, and second, to conduct hydrofracture tests at different overburden pressures. The experiments were defined as LS1 through LS5. LS1 to LS3 were carried out with only the sand as the test medium, while LS4 and LS5 were completed in the layered sand and Granular A soils.

The sand and Granular A materials were placed in 300mm thick loose lifts, which were then mechanically compacted using a light-duty vibratory compactor to at least 95% of the standard Proctor maximum dry density (as determined prior to placement). Throughout the course of the experiments, the relative density and the moisture content of the two materials were measured with a calibrated nuclear density gauge at the four corners and the centre of the test pit. The probe rod of the nuclear gauge was set to penetrate into the sand a depth of 150 mm and the gauge was kept at least 0.5 m from the sidewalls, to reduce the potential for interference. Following the compaction tests, the probe holes were refilled with sand and compacted further to minimize the formation of any possible flow paths through discontinuities. The measured relative densities of the sand material during placement ranged from 1668 to 1786kg/m^3, though most readings were close to 1740kg/m^3. All of the measured densities of the sand material were within 5% of the standard Proctor maximum dry density (1742.8kg/m^3). The water content of the sand material was measured to vary from 4.2 to 6.7%, which was within 2% ± of the optimum water content. For experiments featuring the Granular A, the dry densities and moisture contents for this material ranged from 2026 up to 2074kg/m^3, and 6.8 to 7.6%, respectively.

3.2 BOREHOLE CONSTRUCTION

The borehole was advanced through the steel plate (bulkhead) bolted to the narrow end of the pit. The bulkhead separated the smaller pit used to conduct these experiments from a much larger test facility where the source of drilling fluid and displacement pump were located. The opening of the bulkhead was 200 mm in diameter, and was further reduced by the placement of a Lexan sheet with a 60 mm diameter opening cut through its centre. The borehole was positioned at a depth of 750 mm from the ground surface of the soil.

The borehole diameter was 50 mm, and was located 1m, (approximately 35 borehole radii), from the sidewalls. It was expected that this distance was sufficient to eliminate the impact of the sidewall boundaries (this was later confirmed by the three dimensional finite element analysis work of Xia, 2008)). The borehole was advanced using a hand soil auger specifically designed for excavation in cohesionless materials to a depth of 1.5 m into the sand. The auger was removed and cleaned every 300 mm to prevent overfilling and excessive cuttings within the open borehole.

The scale of the model is considered to be consistent with small diameter installations of fibre optic cables or pressurized gas or water conduits.

3.3 PRESSURE APPLICATION

An inflatable packer was then placed into the borehole to seal the borehole during the application of the drilling fluid. The packer measured 1.2 m in length and had a diameter of 50 mm. The packer was inserted into the borehole to a depth of 1.0 m. The remaining portion of the packer gland was used to seal the end of the borehole with the bulkhead once inflated. The packer was inflated using a pressure regulated Nitrogen gas.

The internal fluid pressures were applied to the borehole using a pre-mixed Bentonite based drilling slurry and a pre-primed displacement pump, both commonly used in the drilling industry. The displacement pump was powered using a four stroke gas powered engine coupled with a centrifugal clutch. Once the clutch was engaged, the fluid application through the packer commenced immediately. The drill fluid was pumped through the sealed packer into the borehole using pressure resistant hosing and quick release fittings tested up to 1350 kPa (200 psi). The internal fluid pressure was permitted to gradually accumulate during application over the course of 30 seconds to a minute at which time, mud loss would typically occur at the ground surface. Once mud flow with the surface of the test cell had been established, the engine was shut off and the pump was disengaged halting further flow into the borehole.

The internal mud pressure was monitored using a resistance pressure transducer with the signal cable fed out through the centre of the packer to a data acquisition system. The packer and pressure transducer were capable of resisting or monitoring pressures up to 6500 kPa (RocTest, 2007) and 2400 kPa respectively.

3.4 SURFACE MONITORING

In order to monitor the surface displacements of the soil during loading, a grid spaced at 0.5 m intervals was painted on the surface of the sand or the Granular A providing control points for locating wooden blocks which acted as displacement monitoring targets, as shown below in Figure 2. The targets were placed at 0.25 m intervals on the ground surface, staggered so that movement of any one target did not result in interruption of the view of other targets behind. Stationary (or fixed) targets were painted on the concrete walls of the pit so that, should a camera move during the experiment, the displacement of the camera could be determined by tracking the movement of the fixed targets. Additional lighting was also provided to minimize errors resulting from the movement of shadows or shifts in the natural light.

The ground surface displacements were calculated by interpreting images captured using two, 10.1 mega-pixel Canon Eos Rebel XTi cameras fitted with 28 to 90 mm standard zoom lenses at two orientations. A MatLab based displacement tracking system was used to interpret the displacements of the soil surface, namely the Particle Image Velocimetry software GeoPIV of White et al. (2003).

One camera was placed on a fixed concrete structure independent of the test soil, positioned to capture displacements axially along the length of the borehole facing the end wall. The second was positioned on the ground surface of the test soils to capture displacements across the length of the borehole. The two cameras were programmed to capture images at four second intervals, and then the images were uploaded directly to a personal computer (PC) for storage. Using the known dimensions of the fixed objects within the images, the displacement in millimetres was calculated at each target block in the horizontal (x or y) and vertical (z) directions.

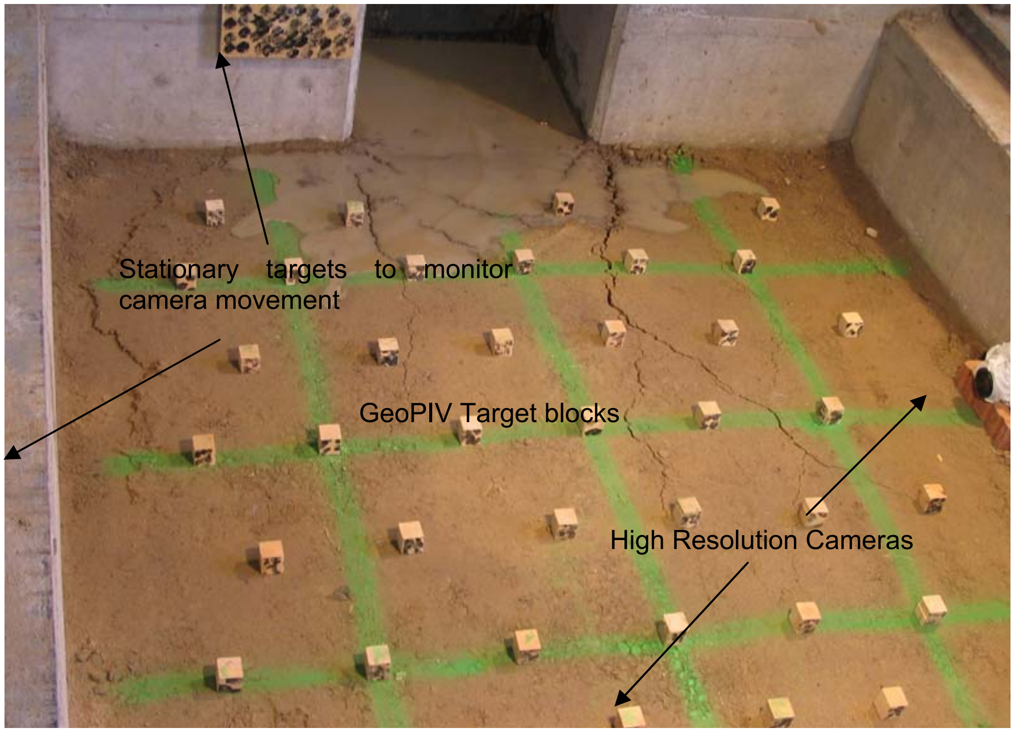

Figure 2 Configuration of GeoPIV cameras and targets

4. EXPERIMENTAL RESULTS

4.1 MAXIMUM INTERNAL FLUID PRESSURES

The measured maximum internal pressures from experiments LS1, LS2 and LS3 were respectively found to be 75.6, 81.1 and 94.6 kPa, corresponding to a maximum percent difference between the three experiments of 22%. The maximum internal mud pressures that were measured during the two layered experiments (LS4 and LS5) were observed as 132.3 and 150.5 kPa respectively, corresponding to a percent difference of roughly 6%. The results of the maximum internal mud pressures measured during all of the experiments are provided in Table 1. An image of the ground surface typical for the sand experiments following fluid loss is shown below as Figure 3.

Test Identification	Estimated σ_{vo} (kPa)	Internal p_{max} (kPa)	FEA Results (kPa)	Delft Solution (kPa)	Yu & Houlsby (kPa)	Carter, Booker & Yeung (kPa)
LS 1 - Sand	12.8	94.6	74.0	97.7	207.8	199.3
LS 2 - Sand	12.8	81.1	74.0	97.7	207.8	199.3
LS 3 - Sand	12.8	75.6	74.0	97.7	207.8	199.3
LS 4 - Layered	14.1	132.3	130.1	101.6	214.3	209.7
LS 5 - Layered	14.1	150.5	130.1	101.6	214.3	209.7

Table 1 Experimental results and various analytical solutions

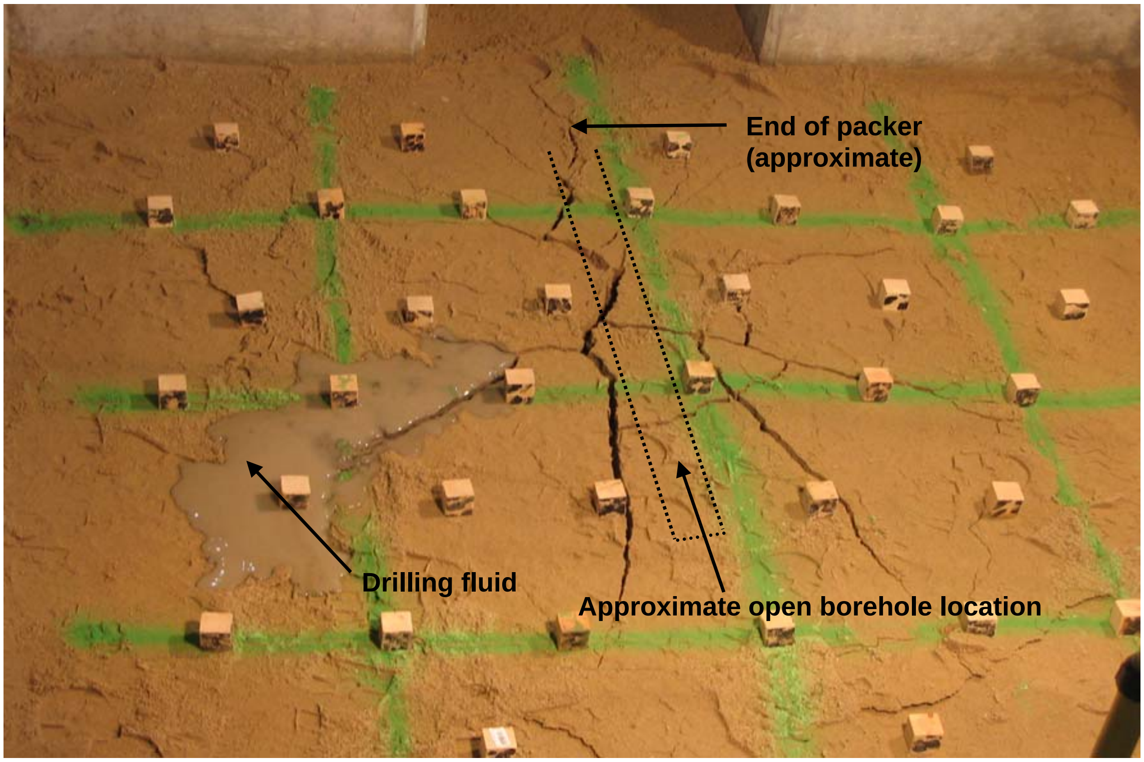

Figure 3 Mud loss following loading of LS1 – sand only

4.2 SURFACE DISPLACEMENTS

The surface heave observed during the sand tests was found to vary from 8.7 to 43.8 mm though was typically around 25 to 27 mm along the centreline of the borehole. The horizontal displacements in both lateral directions were found to vary from 3 to 25 mm though were typically around 15 to 22 mm. The final results indicate that the ground showed near vertical heave along the centreline of the borehole. The displacements tapered down to near zero with distance from the centreline of the borehole. Quiver and contour images of a representative experiment are shown as Figures 4a and 4b.

The volume of the displaced material was calculated from the three dimensional images following calculation of the overall displacements for the single layered experiments. The fluid volumes ranged from 6.7 to 24.1 litres for tests LS1 to LS3 and as 20.2 and 43.6 litres for LS4 and LS5 respectively.

An incremental volume change was calculated for LS1 to try to determine how the displacement occurred with time of application. At a time approximately 12 to 15 seconds before the fluid breach of the ground surface, (approximately 1/2 of the experimental time) approximately 1/3 of the total displacement had occurred. The time reference used for the volume calculations assumed that the breach of the ground surface corresponds with the maximum observed fluid pressure.

The surface displacements monitored during LS4 and LS5 were found to be very similar to those observed in the experiments carried out in the sand only. The maximum observed surface displacements for the layered experiments were found to vary from 25 to 27 mm in the vertical direction and from 5 to 22 mm in both horizontal directions (lateral ground movements).

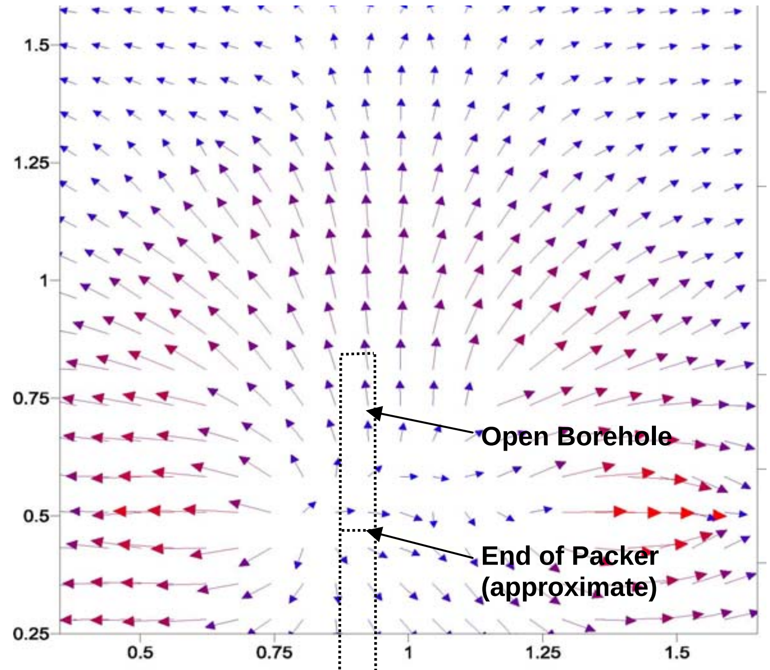

Figure 4a Resultant quiver diagram LS1 - Sand only

Note: All dimensions in metres; total volume of displaced soil is 6.7litres.

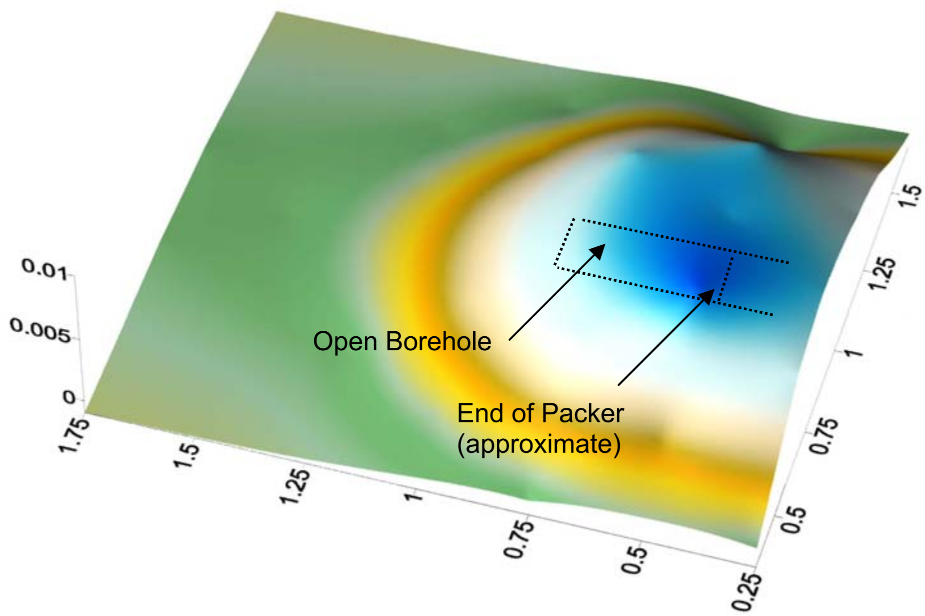

Figure 4b Resultant contour diagram LS1 – Sand only (all dimensions in metres)

The most distinct difference was in the total size of the area of the soil impacted by the loss of drilling fluid at the ground surface. In tests LS4 and LS5 the zone of the surface that experienced cracking and heave was significantly greater than areas observed in the uniform sand tests. The area impacted by the ground failure was contained mostly to a radius of around 400 mm or less, whereas the radius of influence in the sand and gravel was found to displace as a mass and form a shallow mound on the surface over the centreline of the borehole.

The movement of the drilling fluid to the surface of the layered material did not necessarily occur above the centreline of the borehole. It is believed that the drilling fluid ‘pooled’ beneath the granular layer and as pressure accumulated, the drilling fluid naturally sought the path of least resistance which would have been the thinnest and/or the least compact section. Though the Granular A was essentially cohesionless, the permeability of the underlying sand was slightly higher than the GW-SW layer. The coefficient of permeability of the sand was measured from the laboratory tests to be approximately 3.2×10^{-3} cm/s while the typical k value is around 1×10^{-4} cm/s for a well graded Granular A material (Holtz and Kovacs, 1981, OPSS 1010, 2004). The difference between the two k values was enough to allow the fluid to pool and travel horizontally below the sand and gravel until a breach of the surface could be completed. The ‘pooling’ of the drilling fluid was observed to some extent during the excavation process where the upper 25 to 50 mm of the underlying sand was infiltrated with drilling fluid as a path was formed to the ground surface. The granular layer immediately above the ‘pool’ was not always infiltrated by the drilling fluid, and in fact, in most cases once failure had occurred and flow to the ground surface had been established, the volume of infiltrated granular material was very small.

5. ACTUAL VERSUS THEORETICAL INTERNAL FLUID PRESSURES

The results of a two-dimensional plane strain finite element analysis (FEA) using the program AFENA (Carter, 1992; Moore, 2005) considering a borehole pressure applied radially to the walls of the borehole and a low cohesive frictional material with no filtercake, was calculated as 74 kPa. The percent differences between the experimental results and those calculated during the FEA were found to be 2, 9 and 24%. Comparison of the FEA results with the average peak pressure obtained from the sand only experiments (83.8 kPa) results in a difference of approximately 12%.

Comparison of the Delft solution (Keulen et al., 2001) shows that blowout is estimated to occur at a maximum internal pressure of 97.7 kPa or percent differences of 3.2, 18 and 25% when compared to LS1 through LS3 respectively. The average of the three sand only experiments results in a percent difference of approximately 15% when compared to the Delft solution. Application of the cavity expansion theory developed by Yu and Houlsby (1991) suggest a maximum internal pressure of 207.8 kPa or percent differences of approximately 75, 88 and 93% when compared to the observed peak internal pressures and 85% when compared to the overall average of the three experiments. The last cavity expansion solution that was considered was developed by Carter et al. (1986). This solution results in a maximum internal pressure of 199.3 kPa or percent differences of 71, 84 and 89% when compared to the observed maximum internal pressures. The difference between the calculated and average peak pressure is approximately 82%.

The maximum internal pressure estimated by the two-dimensional FEA considering a layered sand and Granular A configuration was 130.1 kPa which corresponds to percent differences of 1.7 and 14.5% when compared to the results of LS4 and LS5 respectively. Comparison of the FEA results with the average peak pressure obtained from the layered experiments (141.4 kPa) results in a percent difference of around 8%.

The results for the maximum internal pressures calculated by the Delft solution, Yu and Houlsby (1991) as well as by Carter et al. (1986) were determined by assuming a composite material by applying a weighted average unit weight, cohesion and angle of internal friction. Though the assumption of a composite material is a simplification, this is considered a reasonable first approximation for consideration of a two–material system.

Calculation of the maximum internal pressure assuming the Delft solution results in an internal pressure of 101.6 kPa or percent differences of 26 and 39%. The average of the two layered experiments results in difference of approximately 33% when compared to the Delft solution. The cavity expansion theory presented by Yu and Houlsby (1991) results in a peak internal pressure of 214.3 kPa corresponding to percent differences of 47 and 35% or 41% when compared to the average peak pressure. Finally the cavity expansion theory developed by Carter et al. (1986) results in a maximum internal pressure of 209.7 kPa or percent differences of 45 and 33% respectively and 39% for the average peak pressure.

6. ACTUAL VERSUS THEORETICAL GROUND DEFORMATIONS

The displacement results of the two-dimensional FEA were then compared to those observed during tests LS1 through LS3. Typical displacements reported by the numerical analysis ranged from 2 to 3 mm, with the upper limit observed with increasing soil density. When compared to the observed displacements of around 25 mm, the observed deformations were about 9 times the calculated values. Comparison of the layered materials faired worse as the ground surface displacements estimated by the FEA model were around 1.5 to 2.5 mm and the horizontal displacements were negligible. The observed vertical displacements were about 12 times the calculated values.

The source of this error is likely based in the fact that the FEA models the application of the drilling fluid as a pressure on the surface of the borehole, and does not model the physical volume of mud moving into the soil surrounding the borehole. In the experiments, the application of the drilling fluid contributes additional volume to the soil mass, and it appears that this results in most of the surface displacements. Another possible source of error may be that for a FE model to be valid, it is assumed that the material being modelled is continuous (either a solid mass or highly fractured throughout). Clearly it can be seen from the photographs that the cracking resulting from the borehole pressurization is concentrated to a small area, and consequently the material within the cracked zone is no longer a continuum.

Based on these results, it is clear that a finite element numerical analysis cannot be used to describe the surface deformations in HDD applications. Further research is required to develop a suitable numerical model to accurately represent the deformations resulting from the application of a drilling fluid.

7. CONCLUSIONS

Based on the results of the hydrofracture experiments, it can be concluded that within a relatively loose to compact sand material as well as in the layered soil profile considered in these experiments, the hydrofracture failure occurs above the centreline of the borehole. The assumption of the nature of the borehole failure is based on the observations of the soil around the borehole that was affected by the drilling fluid.

The filtercake that formed generally had uniform thickness extending approximately 2 to 4 borehole diameters around the borehole, though changes in shear strength as a result of mud penetration into this zone may have been negligible. The maximum displacements typically occur immediately above the centreline with a relatively large area impacted in terms of soil disturbance and surface cracking.

The maximum internal mud pressures are well estimated employing either the solution described by Lugar and Hergarden (1988) or the Delft solution (Keulen et al. 2001) or a finite element analysis model with reasonably accurate soil parameters. The solutions outlined by Yu and Houlsby as well as by Carter et al. (1986) were found to overestimate the maximum internal pressures significantly. When the finite element analysis was used to estimate the displacements at the ground surface, it was found that the maximum vertical heave was significantly underestimated.

8. ACKNOWLEDGEMENTS

The work was supported with funds from the Natural Sciences and Engineering Research Council of Canada. The contributions of Hongwei Xia, Mark Talesnick and Graeme Boyd to these experiments are greatly appreciated.

REFERENCES

Bowles, J.E. (1995). *Foundation Analysis and Design*. *Fifth Edition*. McGraw-Hill, New York, New York. page 100.

Canadian Geotechnical Society. (2006). *Canadian Foundation Engineering Manual (CFEM). Fourth Edition*. Technical Committee of Foundations, Richmond, British Columbia. pages 13-19.

Carter, J.P. (1992). *PROGRAM AFENA: A general finite element algorithm*, University of Sydney.

Carter, J.P., Booker, J.R. and Yeung, K.S. (1986). *Cavity expansion in cohesive frictional soils*. Geotechnique, Vol. 36(3): 349-358.

Conroy, P. J., Latorre, C. A., and Wakeley, L. D. (2002a). *Installation of fiber-optic cables under flood-protection structures using horizontal directional drilling techniques*. ERDC/GSL TR-02-8, Geotechnical Structures Laboratory, Vicksburg, MS.USACE.

Conroy, P. J., Latorre, C. A., and Wakeley, L. D. (2002b). *Guidelines for installation of utilities beneath Corps of Engineers levees using horizontal directional drilling*. ERDC/GSL TR-02-9, Geotechnical Structures Laboratory, Vicksburg, MS. USACE.

Hefny, A., Lo, K.Y. (1992). The interpretation of horizontal and mixed-mode fractures in hydraulic fracturing tests in rocks. Canadian Geotechnical Journal, Vol. 29: 902-917.

Holtz, R.d., Kovacs, W.D. (1981). *An Introduction to Geotechnical Engineering*, Prentice Hall, Toronto, page 210.

Keulen, B., Arends, G., Mastbergen, D.R. (2001). *Maximum allowable pressures during directional drillings focused on sand*. Delft Geotechnics Thesis Paper: 23-32, Appendices 39-74.

Latorre, Carlos A., Wakeley, Lillian D., and Conroy, Patrick J. (2002). *Guidelines for installation of utilities beneath Corps of Engineers levees using horizontal direction drilling*. Geotechnical Structures Laboratory, Vicksburg, MS. USACE.

Lugar H.J., Hergarden H.J.A.M. (1988). *Directional drilling in soft soil; influence of mud pressures*, Proc., ISTT-No Dig, 1998, Washington D.C., Paper 6B: 1-7.

Moore, I.D. (2005). *Analysis Of Ground Fracture Due To Excessive Mud Pressure,* No-Dig 2005, Orlando, Florida.

Ontario Provincial Standards Specification - 1010. (2004). *Material specifications for aggregates – base, subbase, select subgrade and backfill material*. Ontario Provincial Standards, Vol. 2(1010): 1-15.

RocTest Canada. (2007). *Technical specifications – high-pressure packers*. website, www.roctest.com

Van Brussel, G.G., Hergarden, H.J.A.M. (1997). *Research (CPAR) program: Installation of pipelines beneath levees using horizontal directional drilling*. SO-59407-701/2. Department of Foundations and Underground Engineering, Delft Geotechnics, 1-16.

Vesić, A.S. (1972). *Expansion of cavities in infinite soil mass*. ASCE Journal of the Soil Mechanics and Foundations Division, Vol. 98: 265-290.

White D. J., Take W.A., Bolton, M.D. (2003). *Soil deformation measurement using particle image velocimetry (PIV) and photogrammetry*. Geotechnique, Vol. 53(7): 619-631.

Yu, H.S., Houlsby, G.T. (1991). *Finite cavity expansion in dilatant soils: loading analysis*, Geotechnique, Vol. 41(2): 173-183.

Yu, H.S. (2000). *Cavity Expansion Methods in Geomechanics*. Kluwer Academic Publishers, 65-73.

Xia, H.-W. (2009) *Investigation Of Maximum Allowable Mud Pressure Within Sand And Clay During Horizontal Directional Drilling,* PhD Thesis, Department of Civil Engineering, Queen's University, January.